

Pixel-Based Skin Detection for Pornography Filtering

A. Abadpour and S. Kasaei

Abstract: A robust skin detector is the primary need of many fields of computer vision, including face detection, gesture recognition, and pornography filtering. Less than 10 years ago, the first paper on automatic pornography filtering was published. Since then, different researchers claim different color spaces to be the best choice for skin detection in pornography filtering. Unfortunately, no comprehensive work is performed on evaluating different color spaces and their performance for detecting naked persons. As such, researchers usually refer to the results of skin detection based on the work done for face detection, which underlies different imaging conditions. In this paper, we examine 21 color spaces in all their possible representations for pixel-based skin detection in pornographic images. Consequently, this paper holds a large investigation in the field of skin detection, and a specific run on the pornographic images.

Keywords: Pornography Filtering, Skin Detection, Content-Based Image Retrieval, Color Modeling, Color Image Processing.

1 Introduction

With the rapid penetration of the Internet into every part of our daily life, it is agreed that it will be an important media for future communication, perhaps even more important than the television [1]. In 1996, it was estimated that the Internet was grown into an international network, connecting over 60 million users in more than 60 countries [2].

Though, it is proved that even for non-regular users of the Internet it is getting more and more contaminated with harmful content, such as pornography, violence, hatred and the forth. In a recent survey, one in four kids reported having at least one unwanted exposure to sexually explicit pictures during the past year, and one out of five reported receiving a sexual solicitation [3]. Also, an early investigation by a university student showed that approximately 83% of the images in the Usenet groups were pornographic (in 1995) [4]. Recent statistics reveal that 25% of the queries in search engines, 8% of emails, and 12% of homepages are porn-related [5,6] (see [7] for more statistics and [8, 9, 10, 11] for more details on the impact of the issue).

While parents and educators tend to have more control on the information exposed to their children when

surfing the web [12], the conventional textual approaches (such as NetNanny, CyberSitter, and SurfWatch) are not performing well [13]. While failing to give enough immunity, the text-filtering approaches also blocks many useful sites; just because of the presence of some certain phrases. For example, a commercial package blocked the White House children's page in 1996 [14]. On the other hand, the owners of the harmful sites are inventing new methods for shutting down the text-searching immunity systems. Approaches like only-picture pages and safely-named files are now just common. Consequently, in the recent years the pictorial content-based filtering is gathering more and more attention.

To have an idea about the importance of the images for content-based internet filtering, it is useful to review the results of a recent survey. The statistics of more than 4,000,000 HTML pages reveal that more than 70% of them contain images [15]. Also, the results show that a single HTML file, averagely contains 18.8 images [15]. The statistical review of 1,232 pornographic and 6,967 non-pornographic webpages reveals that 72% of pornographic webpages have more than 5 images and 60% of them have more than 10 images [16]. Also, 40% of pornographic webpages have more than 5 links to image and video files. Hence, the ability to detect pornographic images is a useful tool towards filtering adult pages in the Internet.

One should be aware that the exact definition of an erotic image differs in different countries and different cultures. The exact definition of pornography is even

Iranian Journal of Electrical & Electronic Engineering, 2005.
Paper first received 24th April 2005 and in revised form 11th March 2006.

A. Abadpour is a Msc student at Mathematics Science Department, Sharif University of Technology, Tehran, Iran. S. Kasaei is with the Computer Engineering Department, at the same university.
E-mail: abadpour@math.sharif.edu, skasaei@sharif.edu.

undefined in less-conservative countries. For example, in UK there are seven acts of parliament concerning pornography [17], but in US, the Communications Decency Act was ruled unconstitutional in June 1997 and its successor, the Child Protection Act is subject to legal challenge. This subject is out of the scope of this paper and the interested reader is referred to [18,19, 20, 21]. As such, we agree with the authors in [22] that "pornography is an ill-defined concept and that we use it loosely, to refer to unwanted material with a sexual content".

Figure 1 shows the number of published scientific papers (either in conferences or journals) devoted to content-based pornography detection. The chart covers the period of 1996 to 2004, because the first known works were published in 1996 (see Section 2-A). This figure depicts the motivation of scientific society to solve the problem of unwanted exposure of pornography in the Internet.

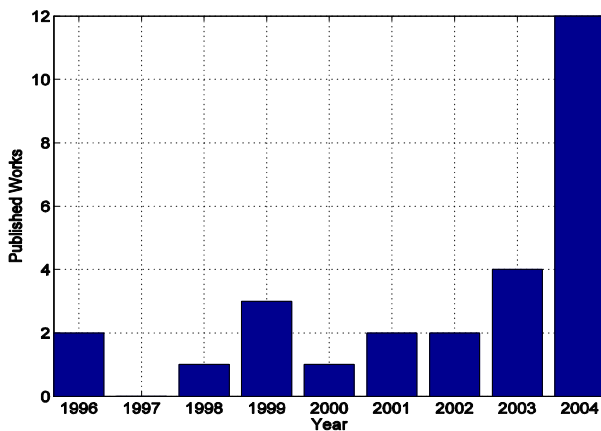


Fig. 1 Number of scientific publications dedicated to content-based pornography filtering in the years of 1996 to 2004.

A rapid review of the available content-based pornography detection approaches (see Section 2-A) reveals that they are all essentially based on detecting skin areas in the images. Also, a more careful review shows that the frequently applied methods for skin detection are pixel-based approaches using ordinary or Bayesian *look-up tables* (LUT).

According to the number of available color spaces and the diversity of the choices made in the literature, it is clear that a thorough investigation of the performance of different color spaces for this problem is mandatory. In this paper, we examine 21 color spaces in all their possible representations. The examination is aimed on evaluating different color modeling approaches in terms of their performance on skin detection in pornographic images.

The following parts of the paper are organized as follows. Section 2 reviews the available pornography filtering (Section 2-A) and the relating skin detection (Section 2-B) literature. This review tends to answer two important questions. Firstly, it is focused on the

importance of the skin detection stage in these approaches. Secondly, it enlists the skin detection techniques, utilized in this literature. Section 3 states the mathematics of pixel-based skin detection methods, and Section 4 describes the datasets used in this research. Section 5 holds the experimental results and finally Section VI concludes the paper.

2 Literature Review

A. Content-Based Pornography Filtering

The first work on classifying nude pictures belongs to Forsyth et. al. [23, 24, 25]. In that approach, firstly, the images containing large areas of skin are detected (using the IRgBy color space) and then using a specially defined human structure [26, 27], the images containing human figures are recognized as the nude ones. In their approach, only the images which are at least covered in one third by the skin area are fed to a geometric analyzer. While all the images used in [23, 24, 25] are 128×192, it takes about six minutes for the method to process a single image. Though, the final recall of the method is less than 50%.

After that, other researchers made new contributions in this field. In [28], the researchers utilized skin detection in the RGB color space equipped with wavelets and central moments on 128×128 images to develop the WIPE™ system.

In [22, 29, 30], the researchers combined the results of a simple skin area estimator based on a skin detection filter with textual analysis results. That paper reports that "while a threshold is selected, the choice of the color space is not critical. This is somewhat surprising because other authors advocate the use of IRgBy". That work was extended in [31] using a specific neural network to raise the recall rate up to 90%. The researchers draw the final conclusion that "provided that enough training data and a histogram-based representation of the color distribution are used, then the choice of color space is not critical" [31].

In [32], the authors describe the steps towards developing an adult image detection scheme using the skin color in the YUV, YIQ, and their polar representations (YUV°, YIQ°). In that approach, a Sobel edge detector and a Gabor filter judged the results of the skin detector. In [33] the researchers used the CIE-Lab color space for detecting the skin areas in the images. The results were then analyzed using some geometrical features.

In [34], the researchers computed some shape descriptors using the results of skin tone detection in the YCbCr and IRgBy (25) color spaces. Then, using an Adaboost learning scheme, the erotic images were classified. In [35], the researchers combined the results of a neural network classifier working on image features with a commercial text-filtering tool developed by SurfWatch (used by Altavista). The image feature used in that work only related to the portion of pixels identified to be skin (in the RGB color space), with no

further geometric processing.

The skin detector in [36] was used in [37, 38] to develop a MPEG7-based adult image identification system, using query-based search into an erotic dataset. In the approach described in [39] the results of a skin detector in the RGB and HSV color spaces were used to produce other features like a simple texture descriptor. Then, all of the features were fed to a *state vector machine* (SVM). In [40], the researchers used the results of a straight skin-detection rule ($R > G$ or $R > B$) with a SVM classifier. In [41, 42] the researchers gave general cues for developing a web-filtering tool.

In [43], a Gaussian mixture model was equipped with Bayesian inference to utilize the skin detection stage. Then, the results were fed to a SVM. In [44], the researchers utilized genetic algorithm for locating the loci of nude pictures in a search space containing huge 801-D feature vectors. Each feature vector contained color histograms in the Cb and Cr color components plus some shape descriptors. Alongside using the histograms of color components in the feature vector, the method in [44] devised hard thresholds on the Cb and Cr components to extract the skin-like objects ($78 < C_b < 135$, $85 < C_r < 185$). In [45, 46], the researchers used the results of a skin detector in the RGB color space for a multi-layer perceptron classifier. In the extended works they applied a better skin detection filter developed in [36] (see also [47, 48, 49, 50]). In [51] researchers utilized a custom non-linear color space. In [52] a multi-Baysian skin detector was utilized. The information about the available pornography filtering approaches are listed in Table 1.

B. Skin Detection

From the review in Section 2-A, it is clear that it is generally accepted that the first step towards finding the whole human body (or its parts) is to find those parts of the image holding pixels corresponding to the skin material. This assumption is theoretically backed by models of the skin tissue. As such, it is argued that the skin color of human is created by a combination of blood (red) and melanin (yellow, brown) [53]. Most researchers presume from these evidence that the skin color can be recognized in an image with no explicit knowledge about the lighting conditions, the camera calibration, and the subject properties such as the race. A skin detection system consists of two major parts. First, there should be a proper model for representing colors; what we call the color space. Second, there is an inference methodology to obtain information from available skin samples and to extrapolate the results to the given samples. For the first part, Table 2 shows that the solution of different researchers seems to be more related to personal taste rather than experimental evidences [54]. We will discuss this point with more details in this paper.

While there are plenty of methods for modeling and detecting skin tone, as Table 1 shows, in the

pornography detection field, researchers tend to gather around two major choices.

Table 1 Summary of the available pornography detection works.

Work	Used Color Space	Skin Detection Approach
[24, 25, 23]	IR_gB_y	Ordinary Look-Up Table
[28]	RGB	Ordinary Look-Up Table
[22, 29, 31, 30]	RGB, HSV, IR_gB_y , Nrgb	Baysian Look-Up Table
[32]	YUV, YIQ, YUV° , YIQ°	Ordinary Look-Up Table
[33]	CIE-Lab	Not Available
[34]	YC_bC_r , IR_gB_y	Ordinary Look-Up Table
[35]	RGB	Ordinary Look-Up Table
[37, 38]	RGB	Histogram-Based
[39]	RGB, HSV	Ordinary Look-Up Table
[40]	RGB, HSV, IR_gB_y , NRGB, YC_bC_r	Ordinary Look-Up Table
[43]	RGB	Baysian Look-Up Table
[44]	C_bC_r	Ordinary Look-Up Table
[45, 46, 47, 48, 49, 50]	RGB	Ordinary Look-Up Table
[51]	Custom	Baysian Look-Up Table
[52]	RGB, RGB^T	Baysian Look-Up Table

Table 2 Diversity of color spaces utilized for skin detection. The color spaces are defined in Appendix A.

Work	Color Space
[36, 55, 56, 57, 58, 59, 60, 61, 29, 62, 63, 64, 30, 31, 22, 52]	RGB
[61, 65, 66, 67, 68, 69, 70, 71, 72, 73, 74, 75, 76, 77, 29, 31, 78, 79, 80, 40, 81, 82, 83, 30, 22]	HSI, HSV, HSI^c , HSV^c , HLS
[84, 81, 85, 86]	CIE-XYZ
[68, 69, 70, 79, 87, 88, 89, 90, 91, 92, 93, 61, 40, 78, 94, 95, 96, 97, 80, 98]	YC_bC_r
[68, 69, 70, 79, 99, 100, 98, 78, 101, 81, 33]	CIE-Lab
[102, 103, 61, 56, 104, 32, 78, 105, 32, 106, 81, 107, 108, 109]	YIQ , YIQ° , YUV , YUV°
[98, 68, 69, 70, 79, 99, 100, 78, 98, 81]	CIE-Luv
[25, 24, 26, 27, 23, 40, 68, 79, 31, 29, 22, 30]	IR_gB_y , $IR_gB_y^+$
[110, 111, 112, 113, 114, 115, 116, 117, 118, 119, 120, 98, 121, 122, 40, 77, 123, 124, 61, 68, 79, 81, 82, 125, 31, 29, 22, 30]	Nrgb
[56, 126, 78, 97, 52]	RGB^T
[81, 77, 97]	TSL
[127]	Others

From the 26 available approaches for pornography detection, 16 use ordinary LUT, 7 use Baysian LUT, and only 3 utilize a different approach for skin detection. Hence, here we focus on the two methods for LUT-based skin detection process. As such, the

concentration of this paper is on the best choices for representing color vectors.

Few works are available that compare the performance of different color spaces for skin detection [128, 129, 78, 97, 79, 68, 81, 56, 130], but they are all concerned with face detection approach. As mentioned in [131] "*pixel-based skin detection has long history, but surprisingly few papers that provide surveys ... were published*". for a survey of the available color space comparison works see [131]. We argue that as the conditions for pornography filtering are essentially different from other skin-related fields that allow more-or-less constraints on the imaging conditions, a more precise and focused investigation in this field is needed. The contributions of this paper are in three ways. Firstly, here we use all our samples and training data from available pornography resources. Doing as such, we concentrate on finding the best choice of color space for pornography detection purposes. As such, this research is dedicated to detecting skin tone in pornography images taken in absolutely arbitrary conditions. Secondly, we arrange the largest number of color spaces than can be used in an evaluation. While the available works compare less than 10 color spaces with each other, we gather 21 color spaces in a unique experiment. The third contribution of this work is that we make no preassumptions about the best dimension of color spaces. All available works use the original 3-D color spaces, or cut them into 2-D representations by neglecting the component assumed to be related to the illumination. In contrast, we perform all the experiments on each color space in all its possible 3-, 2-, and 1-D representations. Also, more than computing the performance of different color models for the training and test data, we perform a real skin detection task for a large erotic dataset and evaluate different color spaces in terms of their corresponding results.

3 Proposed Method

Assume that we are working in the general color space $c_1c_2c_3$. Also, assume that c_1 , c_2 , and c_3 are linearly scaled and biased to give values in the interval $[0, 255]$ (8-bit representation). The pixel-based skin detection approach presumes that there exists a function $P: [0, 255]^3 \rightarrow [0, 1]$ for which, $P(c)$ shows the probability of c belonging to a skin-related area. The function P is also called the *skin probability map* (SPM) [56, 78]. Generally, P is cut by a fixed threshold to obtain a binary LUT.

There are two general approaches for finding P , *ordinary look-up table* (OLUT) and *Baysian look-up table* (BLUT). Section 3-A presents the color spaces included in this investigation, and Section 3-B and 3-C discuss the two methods for computing P . Finally, Section 3-D proposed a method for detecting the skin map using a proper LUT.

Note that some researchers try to code the LUTs using some simple geometric rules [23,72]. For example,

rectangles [132], set of planes [133], and ellipses [134] are being used. We emphasize that those approaches are simplified versions of the general LUT-based skin detection process discussed here. As, for explaining the skin-tone locus by a set of geometric rules in the color domain, one first should prove that such locus exists.

A. Color Spaces

In this work, we use the 21 color spaces of the RGB, HMMD (as the 3-D space HMM) [135], HSI [136], HSV [137], $I_1I_2I_3$ [138], CIE-XYZ [139], CIE-Luv [139], CIE-Lab [139], CIE-LHC [139], $YCbCr$ [140], YIQ [141], YUV [142], IR_gB_y [143], $IR_gB_y^+$ [143], Nrgb [122], YUV [32], YIQ [32], YCbCr [32], HSI^C [77], HSV^C [77], RGBr [126], and TSL [81]. To make the range of different color spaces comparable, they are all normalized to the $[0, \dots, 255]$ interval. See Appendix A for the formulation of different color spaces and the normalization scheme.

An arbitrary color space $x_1x_2x_3$ may be seen in 7 representation of $x_1x_2x_3$, x_1x_2 , x_2x_3 , x_3x_1 , x_1 , x_2 , and x_3 . As such, we examine all possible representations of each single color space. Here, we add the name of the color space before its components (when necessary) to avoid mistakes. For example, the I component in YIQ is called YIQ.I, while the I component in IR_gB_y is called $IR_gB_y.I$. When this is unnecessary, the original names are used, for example I_3 in $I_1I_2I_3$ is easily addressed as I_3 . See Appendix A for a detailed table.

B. Ordinary Look-Up Table (OLUT)

The ordinary LUT-based skin detection approach assumes that the SPM can be estimated from a proper training set. This approach is quite commonly used in the literature (e.g., see [144, 100, 65, 68, 69, 70, 79, 67, 145, 35, 44, 34, 32, 48, 49, 50, 45, 46, 47, 39, 28, 24, 25, 23]).

Here, we investigate the validity of this assumption. Assume that we have two sets of 3-D vectors, relating to skin and non-skin (control) areas, respectively. Also, assume that there are N_S pixels deliberately extracted from skin area and N_C pixels which do not represent skin. Both N_S and N_C should be large enough. In our case, we have $N_S=278530$ and $N_C=192514$. Now, assume that H_S denotes the p-D histogram of all skin samples in an arbitrary color space ($p=1, 2, 3$) (H_C is computed for the control dataset in a similar way). By setting different values of p we are able to remove one or two of the components of a color space. For computational purposes we select the number of bins in each direction equal to 16, 64, and 256 for 3-, 2-, and 1-D representations, respectively.

The main assumption behind the validity of OLUT-based skin-detection is that H_S can serve as P , the SPM. As such, for an arbitrary threshold value θ , all color vectors c that satisfy $P(c) \geq \theta$ are regarded as skin samples. Due to the fact that the summation of all elements of H_S equal unity, the elements of H_S may be

too small. Thus, setting $P(c)=H_s(c)$ will result in difficulties in selecting θ . To make the range of feasible values of θ more appropriate, we compute P as:

$$P(\vec{c}) = \frac{H_s(\vec{c})}{\max_{\vec{d}}\{H_s(\vec{d})\}}. \quad (1)$$

Consequently, θ can accept all values in the range of $[0, 1]$ [68].

For an arbitrary value of θ , the OLUT is a binary array with a size similar to H_s and H_c . Zero element in the c bin means that c does not represent skin tone, while unity indicates skin. Then, the *true positive* (TP) and *false positive* (FP) values are computed as:

$$TP = \sum_{\vec{c} \in [0, L]^p} H_s(\vec{c})LUT(\vec{c}), \quad (2)$$

$$FP = \sum_{\vec{c} \in [0, L]^p} H_c(\vec{c})LUT(\vec{c}). \quad (3)$$

Clearly, we expect a value of θ resulting in a TP of around unity and a FP of around zero. Note that FP and TP are always between zero and unity.

For an arbitrary color space and a value of p , by selecting different values of θ in the $[0, 1]$ interval, we compute a set of corresponding (TP,FP) pairs. When these pairs are drawn in an axis, we reach to the *receiver operator characteristics* (ROC) curve. This curve is a keen way to determine an appropriate value of θ .

C. Bayesian Look-Up Table (BLUT)

Assume that a color vector c is given. Note that, what we actually need is $p(\text{skin}|c)$. From the Bayes theory we know that

$$P(\text{skin}|\vec{c}) = \frac{P(\vec{c}|\text{skin})p(\text{skin})}{P(\vec{c}|\text{skin})p(\text{skin}) + P(\vec{c}|\sim \text{skin})p(\sim \text{skin})}, \quad (4)$$

where $p(\text{skin})$ and $p(\sim \text{skin})$ are *a priori* probabilities, which are absolutely unknown. Here, $p(\text{skin})$ and $p(\sim \text{skin})$ are the probabilities that an arbitrary pixel represents skin and non-skin tones, respectively. Now, we write down the Bayes equality for $p(\sim \text{skin}|c)$ as:

$$P(\sim \text{skin}|\vec{c}) = \frac{P(\vec{c}|\sim \text{skin})p(\sim \text{skin})}{P(\vec{c}|\text{skin})p(\text{skin}) + P(\vec{c}|\sim \text{skin})p(\sim \text{skin})} \quad (5)$$

Note that

$$P(\text{skin}|\vec{c}) + P(\sim \text{skin}|\vec{c}) = 1. \quad (6)$$

as trivially expected.

Using (4) and (5) we have

$$\frac{P(\text{skin}|\vec{c})}{P(\sim \text{skin}|\vec{c})} = \frac{p(\text{skin})}{p(\sim \text{skin})} \times \frac{P(\vec{c}|\text{skin})}{P(\vec{c}|\sim \text{skin})}. \quad (7)$$

Here, we define two notations

$$p^-(\vec{c}) = \frac{P(\vec{c}|\text{skin})}{P(\vec{c}|\sim \text{skin})}, \quad (8)$$

$$p^+(\vec{c}) = \frac{P(\text{skin}|\vec{c})}{P(\sim \text{skin}|\vec{c})}. \quad (9)$$

Note that according to (7), we have

$$p^+(\vec{c}) = \frac{p(\text{skin})}{p(\sim \text{skin})} \times p^-(\vec{c}). \quad (10)$$

Using the normalization scheme used in (1), we have

$$\frac{p^+(\vec{c})}{\max_{\vec{d}}\{p^+(\vec{d})\}} = \frac{p^-(\vec{c})}{\max_{\vec{d}}\{p^-(\vec{d})\}}, \quad (11)$$

which eliminates the two unknown probabilities of $p(\text{skin})$ and $p(\sim \text{skin})$. In fact, $p^-(c)$ is computed using two proper datasets of skin and non-skin, and (11) enables us to use it for creating a BLUT. From this point, everything is just similar to what performed in the OLUT-based skin detection process, described in Section 3-B. This approach is used in [22, 29, 31].

D. Skin Map Computation

Assume that we have the p-D color space X in which H is presumed to be a proper LUT for skin detection. Assume that H is a b^p -bin histogram. For the given image I , the process of finding its corresponding SPM is straightforward: compute J , the representation of I in X . Then, for each single pixel c , compute the corresponding bin in H . Now, c represents skin iff the corresponding bin in H holds unity. This process results in the binary image M (M and I are in the same size). For the sake of simplicity, we propose another version of this scenario. For $0 < \lambda < 1$, first compute I_λ as the resized version of I with ratio λ ($\lambda=10\%$ is a proper choice). Then, compute the SPM for I_λ as described above. Lets call the SPM of I_λ as M_λ . Now, up-sample M_λ , with ratio $1/\lambda$, to reach to M (which is the same size as I). According to the performance of MATLAB in processing arrays, and its deficiency in working with "for" loops, the above scheme gives considerably higher speed (about 4 times). The choice of the upsampling method depends on the expected quality of results; for fast evaluation the nearest neighborhood is a proper choice while bi-linear gives smoother results in cost of higher computational complexity.

4 Datasets

Using the *Google* advanced image search with enabled "large size" option and some erotic keywords, 2284 pornographic images were downloaded. Some of the images came from amateur weblogs devoted to pornography. All images are in color, represented in the RGB color space and compressed using the standard JPEG compression with high visual qualities. After

downloading the images from the net, no preprocessing is performed on them. These images formed a dataset of erotic images. Both indoor and outdoor images of single and multiple people with both complex and simple backgrounds are collected in the dataset. It includes photographs of female Hollywood stars, professional photographs of erotic models, amateur pornographic images, and pictures taken in the beach.

When considering the web-pages containing pornographic content, two major categories are recognized. The first one is the group of professional agencies producing and distributing erotic content. These homepages are mostly restricted to members and comply with regarding laws. As described in [146] the main challenge of content-based pornographic image blocking is to put constraints on accidental access to adult content in the Internet. As such, no one may restrict adult motivated users from viewing pornographic content (that comply with the specialized laws) [147]. Hence, the scope of this research does not include these professional sources of pornography. The second place to find adult images in the web, and the dominant one, is the category of homepages produced by amateurs, even teenagers. As the main challenge of the current research is to restrain these sources, all of the images in the erotic dataset are selected from free resources in the Internet. Note that while some of the images accompany copyright hints of professional agencies, they have been pirated and incorporated into free resources, and thus are added to the dataset.

The pornographic images in free homepages are separated into three major categories. Firstly, there are images that are transferred to the web directly from a digital camera. These images contain no further manipulations. Then, there come images that only contain a tag, indicating the source of the image. From the nature of the tags, it is clear that they are added using one of the free batch image editing softwares available in the Internet. The last, and the least frequent, category is the few images containing professional manipulations. These images are those pirated from professional agencies. Figure 2-a shows the share of each category in the erotic dataset. As seen here, almost all images in the erotic dataset are non-edited.

Figure 2-b shows the histogram of the width and the height of the images in the erotic dataset. As seen here, each histogram contains a single peak. As such, the width of the images is averagely 605 with the standard deviation of 196. Also, the height of the images is averagely 676 with the standard deviation of 235. The peaks of the width and height histograms occur in 520 and 685, respectively.

When it comes to the aspect ratio of the images, interesting features are found. For a $H \times W$ images, its corresponding aspect ratio is defined as $\min\{H/W, W/H\}$. As such, we compensate for images captured horizontally, or vertically. Figure 2-c shows the histogram of the aspect ratios of the images in the erotic

dataset. Hence, the aspect ratio of the images of the erotic dataset are mostly gathered about 2/3 and 3/4. As an example, in a digital *Canon A60* camera, the available resolutions are 1600×1200, 1024×768, 640×480, corresponding. These figures all lead to the aspect ratio of 3/4. This fact, empowers the assumption that the free pornographic images in the Internet are just copied from the camera and distributed without any further manipulations.

Another interesting feature of the collected erotic dataset is the compression ratio of the images. Firstly, it should be emphasized that except for the static and animated banners presented in the erotic resources, the dominant file format in this area is the standard JPEG. As Fig. 2-d shows, the images in the erotic dataset are represented averagely by 1.45 bits per pixel with the standard deviation of 0.8 bits per pixel. Also, the peak of the histogram happens at 1.2 bits per pixel.

Figure 2-e illustrates the number of people present in the images of the erotic dataset. Hence, most of the images in the dataset include a single model. Figure 2-f classifies the images into two groups in terms of the existence of at least one face in the images. This categorization is performed to see if face detection may help localizing naked people [43, 33]. Less than one fourth of the erotic images in the dataset contain no faces. This fact implies that using a face detection method may be beneficial.

Figure 2-g shows the separation of the images in the erotic dataset according to the sexual organs present in them. This figure shows that about half of the erotic images do not contain any such organs.

Another categorization of the erotic image dataset comes in Fig. 2-h. This chart shows that about 89% of the images in the erotic dataset are indoor images compared to the minority of 11% outdoor ones.

The skin area of some of the images of the erotic dataset are cropped manually. The cropped images are then resized to 64×64 pixels. As such, a new training dataset of 314 samples is generated, which is called the skin dataset. Another dataset of 106 patches, each containing pixels corresponding to a single material is also produced. The patches are selected manually from images taken by a *Canon A60* digital camera at daylight with flash. This dataset is used as the control data. Figures 3 and 4 show the skin and control dataset, respectively. We emphasize the vast variety of colors related to skin swatches. Some colleagues of us were hardly believing some of the patches shown in Fig. 3 to represent real skin samples. We believe that the main challenge for a proper skin detector is to adopt to all these skin samples, and yet reject non-skin tones. This is mainly caused by the practical situation in which a pornography-related skin detector should work; unconditional images just found somewhere in the Internet.

5 Experimental Results

The experimental results are carried out in a 2046 MB PIV processor using MATLAB 6.5 and image processing toolbox 3.2.

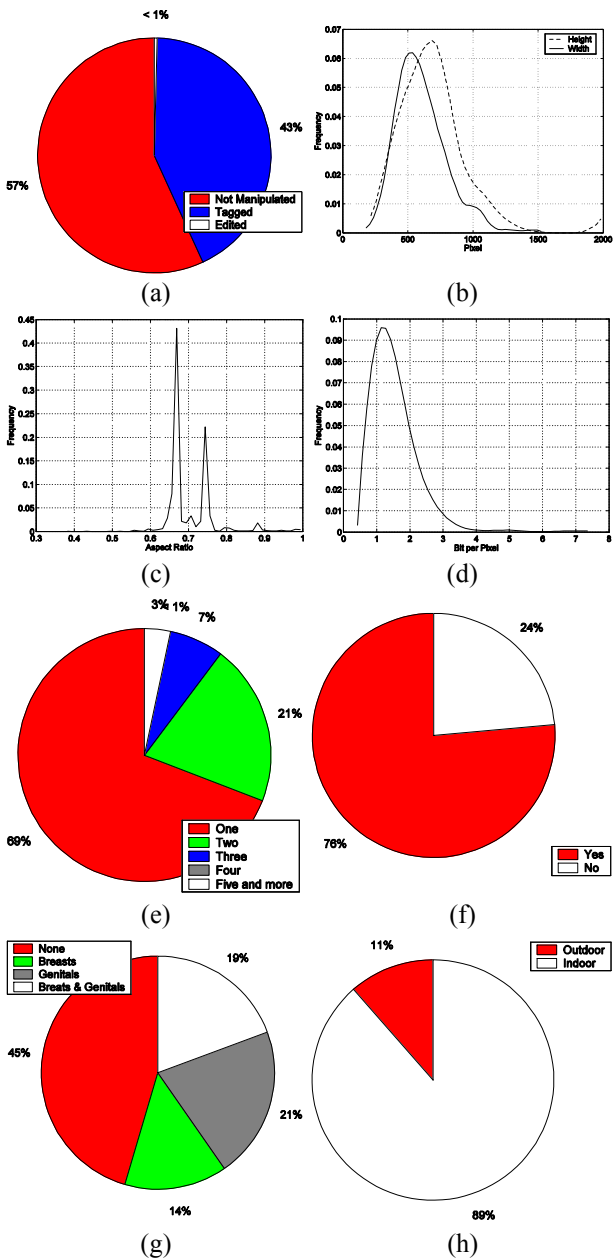


Fig. 2 Statistics of images in our erotic dataset. a) Classification of images into three categories of not manipulated, tagged, and edited. b) Histogram of width and height of images. c) Histogram of aspect ratios. d) Histogram of bpp of images. e) Number of people present in images. f) Is there a face in the image? g) Separation of images according to visible sexual organs. h) Categorization in terms of being outdoor or indoor.

The ROC curves of the OLUT-based skin detector for the 21 color spaces under examination (see Appendix B) reveal several interesting features about the color spaces and their performance in OLUT-based skin detection

processes. Firstly, selecting those color spaces resulting in points in the ROC, satisfying $TP > 90\%$ and $FP < 10\%$, results only in the RGB, HMMD, $I_1I_2I_3$, I_2I_3 , HSI, HSV, HSV.HS, VH, C_bC_r , $Y_cC_bC_r$, IQ, YUV.UV, CIE-Luv, CIE-uv, Nbr, UV, IQ, C_bC_r , HSV^c , HS^c , TSL, TS. Thus, out of $21 \times 7 = 147$ investigated color spaces, only 22 has shown preliminary acceptable results. As such, if a color space is selected by chance, there is only 15% hope that it will be helpful for OLUT-based skin detection purposes. This fact proves that the ongoing investigation is worthy.

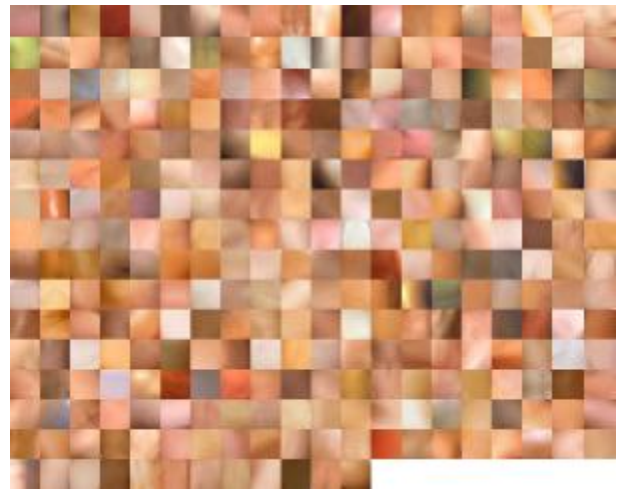


Fig. 3 Samples of skin dataset.



Fig. 4 Samples of control dataset.

Another interesting outcome of the described experiment is the evaluation of the color spaces produced by altering elderly ones. There are six pairs of corresponding color spaces in this experiment. Namely, the (HSI, HSI^c) , (HSV, HSV^c) , $(Y_cC_bC_r, Y_cC_bC_r^c)$, (YIQ, YIQ^c) , (YUV, YUV^c) , and $(IR_gB_y, IR_gB_y^+)$. Figure 5 compares the best achievements of the color spaces in each pair. These are the (HSI, HSI^c) , (HSV, HSV^c) , $(C_bC_r, C_bC_r^c)$, (IQ, IQ^c) , (YUV, UV) , and $(R_gB_y, R_gB_y^+)$. It is clear that none of the manipulated color spaces outperform their regarding ancestors. In fact, the alterations in the structure of more classic color spaces have declined their performances.

An important result of this experiment is that in the YUV, YIQ, and $Y_cC_bC_r$ color spaces, removing the illumination-related component (Y) increases the performance of skin detection process. Thus, the definition of the illumination component in these three color spaces is a good step toward getting invariant to illumination.

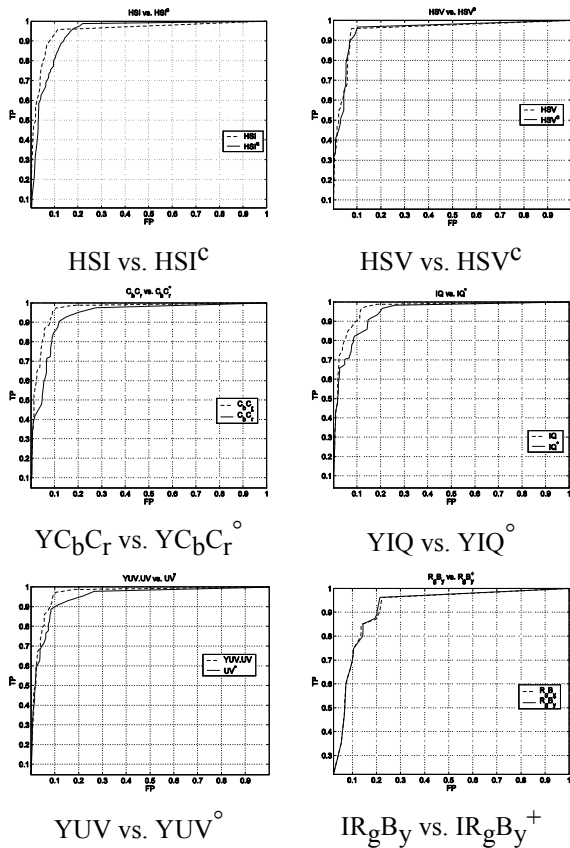


Fig. 5 Comparison of original color spaces with their manipulated versions in terms results of the best combination for LUT-based skin detection processes.

Figure 6 illustrates the best ROC curves obtained from the color spaces in this experiment. We believe that the difference between the performance of these color spaces is not really meaningful. Figure 7 shows the corresponding LUTs obtained in this experiment.

Table 3 lists the resulting true and false positives. We emphasize that further comparison of these LUTs should be based on a larger dataset. Note that as the computation of the LUTs is performed using higher number of bins, there are some TP values less than the preselected margin of 90%. Here, we have used 32 and 256 bins for 3- and 2-D histograms, respectively, to acquire a more precise OLUT.

Selecting those color spaces capable of giving a BLUT satisfying $TP > 90\%$ and $FP < 20\%$, simultaneously, results in CIE-a, CIE-u, Min, HSI.H, R_g , R_g^+ , C_r , C_r^+ , $YI.Q$, Q^+ , YUV.V, and V^+ (see Appendix B). Note that here we have doubled the margin for FP; as the ROC curves tend to fall in Bayesian framework, compared to the OLUT-based one. Also, note that the ROC in CIE-a is visibly outperforming others, even touching the $FP < 10\%$ margin. Note that selecting a color space by chance, there is only a 0.6% chance that it will yield proper BLUT-based skin detection results. Another interesting result of this experiment is that the best color spaces in the Bayesian framework are 1-D ones, compared to the case of OLUT-based skin detection in

which the best 11 color spaces constitute eight 3-D, and three 2-D spaces and no 1-D color space.

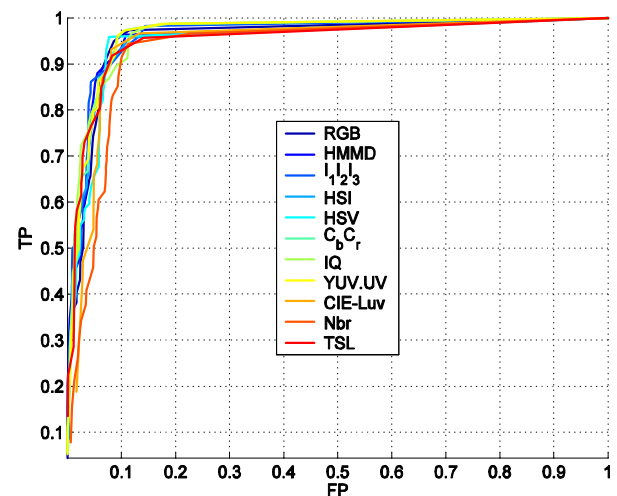


Fig. 6 Best ROC curves for OLUT-based skin detection obtained from investigated color spaces.

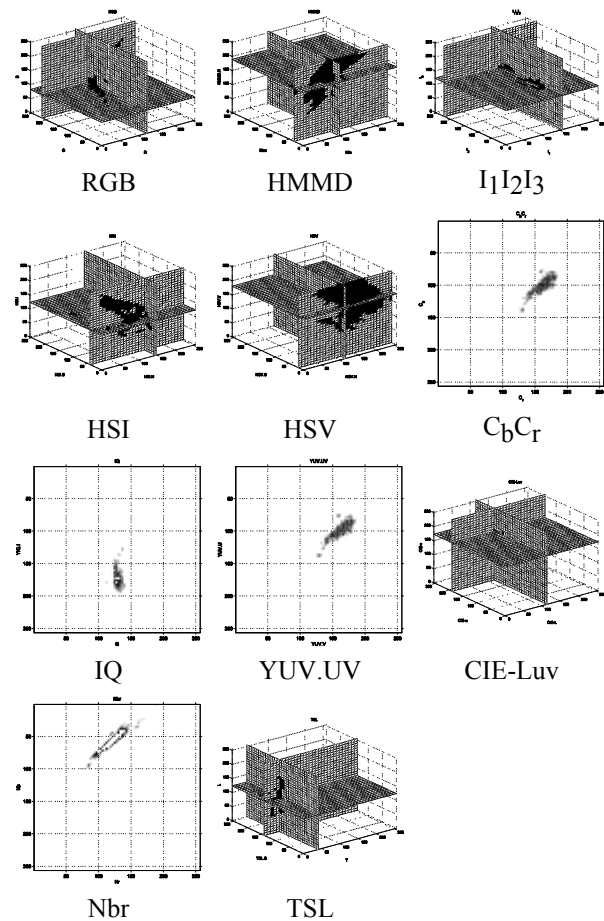


Fig. 7 Best LUTs produced by color spaces under investigation.

Figure 9 compares the best achievements of the color spaces for BLUT-based skin detection in each pair of original and manipulated color spaces. There are six pairs of corresponding color spaces in this experiment.

Namely, the (HSI, HSI°) , (HSV, HSV°) , $(YCbCr, YCbCr^{\circ})$, (YIQ, YIQ°) , (YUV, YUV°) , and $(IR_gB_y, IR_gB_y^{\circ})$. The corresponding pairs of the best combinations are (HSI, H, H°) , (HSV, S, H°) , (C_r, C_r°) , (YIQ, I, Q°) , (YUV, V, UV°) , and (R_g, R_g°) . As visible in Fig. 9, the HSI° performs weaker compared to the HSI. In contrast, the HSV° is far more better than the HSV. The $YCbCr^{\circ}$, YIQ° , and YUV° does not have anything to offer compared to their respective ancestors. The IR_gB_y and $IR_gB_y^{\circ}$ are giving completely the same ROC curves.

Table 3: False and true positive results of the best LUTs produced by color spaces under investigation.

Color Space	True Positive	False Positive
RGB	91%	5.9%
HMMMD	90%	6%
$I_1I_2I_3$	91%	6.3%
HSI	85%	5%
HSV	93%	5.8%
C_bC_r	89%	7.9%
IQ	76%	3.1%
YUV.UV	90%	8.5%
CIE-Luv	91%	7.2%
Nbr	86%	8.7%
TSL	91%	6.4%

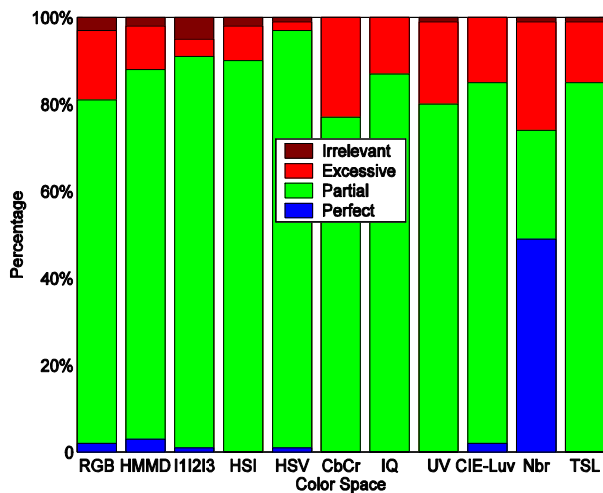


Fig. 8 Results of computing the skin map using the best available LUTs.

Figure 10 compares the ROC curves of the best color spaces for BLUT-based skin detection process. The images in the erotic dataset are processed using the computed BLUTs. Then, the results are separated into the four groups of perfect, partial, excessive, and irrelevant. Figure 12 shows the obtained results. It is clearly visible that the V° and C_r° are dominantly outperforming the others. Comparing Fig. 12 with Fig. 8

reveals that utilizing the Bayesian approach results in a higher rate of correct classification, while it also increases the possibility of irrelevant vectors to be classified as skin. We argue that this occurs when both the nominator ($P(\text{skin}|c)$) and denominator ($P(\sim\text{skin}|c)$) of the fraction $p^+(c)$ get zero, resulting in a non-meaningful value. This fault may be resolved using a better control dataset (which includes more non-skin samples).

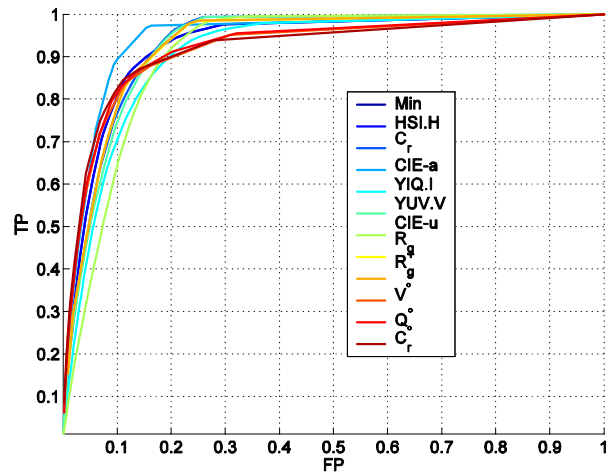


Fig. 10 Best ROC curves for BLUT skin detector obtained from investigated color spaces.

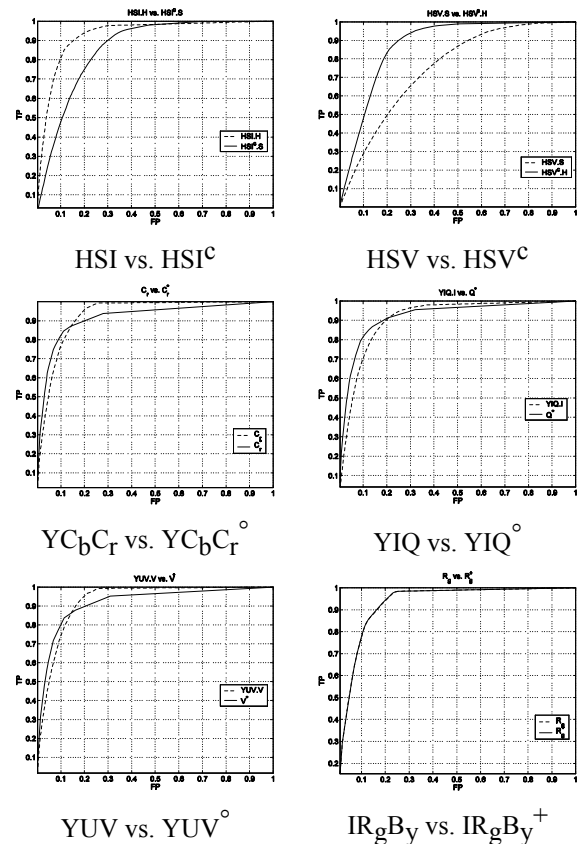


Fig. 9 Comparison of original color spaces with their manipulated versions in terms the results of the best combination for BLUT-based skin detection process.

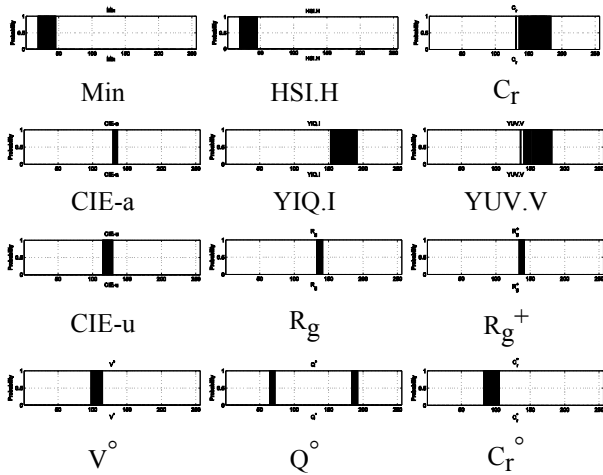


Fig. 11 Best BLUTs produced by color spaces under investigation.

Table 4 False and true positive results of the best BLUTs produced by color spaces under investigation.

Color Space	True Positive	False Positive
Min	85%	13%
HSI.H	85%	13%
C_r	22%	93%
CIE-a	92%	14%
YIQ.I	83%	18%
YUV.V	89%	18%
CIE-u	57%	11%
R_g	78%	16%
R_g^+	74%	13%
V°	92%	28%
Q°	92%	28%
C_r°	95%	32%

Figure 11 shows the best BLUTs produced by the color spaces under investigation. Table 4 lists the resulting true and false positives. We again emphasize that further comparison of these BLUTs should be based on a larger dataset. Note that as the computation of the BLUTs is performed using higher number of bins, there are some TP values less than the preselected margin of 90%. Here, we have used 32 and 256 bins for 3- and 2-D histograms, respectively, to acquire a more precise BLUT. Note that the general results of BLUT-based skin detection are worse than those of OLUT-based skin detection in the training set.

6 Conclusion

In this paper, the 21 existing color spaces are examined for pixel-based skin detection purposes. Each color space is considered in all its seven possible representations. The examination includes measuring

the best performance for classifying the skin pixels in the training dataset plus the real performance in highlighting skin areas in the samples of a large pornographic dataset. Two approaches of ordinary and Bayesian LUT-based skin detection are evaluated. The results shows that the Nbr is the best choice for ordinary LUT-based skin detection. Also, it was observed that the best solutions for Bayesian LUT-based skin detection are 1-D color spaces of V° and C_r° . Utilizing the Bayesian approach is proved to result in higher rate of correct classification, while it also acceptably increases the possibility false positive classification.

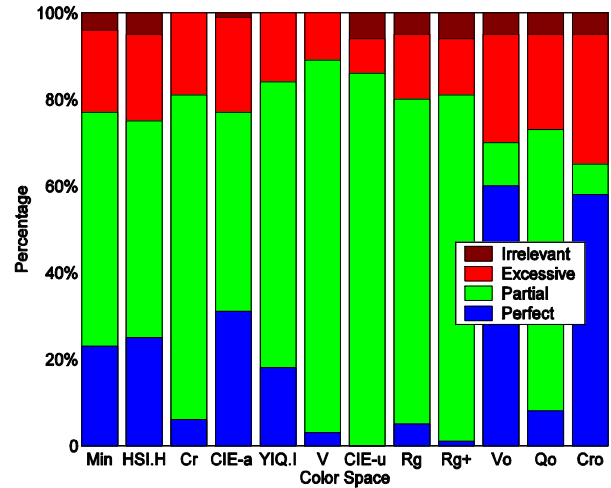


Fig. 12 Results of computing the skin map using the best available BLUTs.

Acknowledgement

During this research, the first authors was partially supported by *Tebian* institute (www.tebian.net). We wish to thank Dr. *Alireza Talebpour* (the head of *Tebian*) from *Shahid Beheshti* university, Iran, and professor *Maria Petrou* from *Surrey* university, Guildford, UK, for their constructive comments and good discussions. Also, we appreciate invaluable aids of *Vahid Vaziri Hamaneh*. The first author also wishes to thank Ms. *Azadeh Yadollahi* for her encouragement and invaluable ideas.

Appendix

A. Color Spaces

The 21 existing color spaces are defined below.

$$HMMD : \begin{cases} H = \cos^{-1} \frac{\frac{1}{2}[(R-G)+(R-B)]}{\sqrt{(R-G)^2+(R-B)(G-B)}} \\ Min = \min\{R, G, B\} \\ Max = \max\{R, G, B\} \\ D = M_2 - M_1 \end{cases} \quad (12)$$

$$HSI : \begin{cases} H = \cos^{-1} \frac{\frac{1}{2}[(R-G)+(R-B)]}{\sqrt{(R-G)^2+(R-B)(G-B)}} \\ S = 1 - \frac{\min(R,G,B)}{I} \\ I = \frac{1}{3}(R + G + B) \end{cases} \quad , \quad (13)$$

$$HSV : \begin{cases} H = \begin{cases} h, B \leq G \\ 2\pi - h, B > G \end{cases} \\ h = \cos^{-1} \frac{\frac{1}{2}[(R-G)+(R-B)]}{\sqrt{(R-G)^2+(R-B)(G-B)}} \\ S = \frac{\max(R,G,B)-\min(R,G,B)}{\max(R,G,B)} \\ V = \max(R, G, B) \end{cases} \quad (14)$$

$$I_1 I_2 I_3 : \begin{cases} I_1 = \frac{1}{3}(R + G + B) \\ I_2 = \frac{1}{2}(R - B) \\ I_3 = \frac{1}{4}(2G - R - B) \end{cases}, \quad (15)$$

$$CIE - XYZ : \begin{cases} X = 0.61R + 0.17G + 0.20B \\ Y = 0.30R + 0.59G + 0.11B \\ Z = 0.00R + 0.07G + 1.12B \end{cases}, \quad (16)$$

$$CIE - Luv : \begin{cases} L^* = 116f\left(\frac{Y}{Y_0}\right) \\ u^* = 13L^*(\hat{u} - \hat{u}_{White}) \\ v^* = 13L^*(\hat{v} - \hat{v}_{White}) \\ \hat{u} = \frac{4X}{X+15Y+3Z} \\ \hat{v} = \frac{9Y}{X+15Y+3Z} \end{cases}, \quad (17)$$

$$CIE - Lab : \begin{cases} L^* = 116f\left(\frac{Y}{Y_0}\right) \\ a^* = 500\left(f\left(\frac{X}{X_0}\right) - f\left(\frac{Y}{Y_0}\right)\right) \\ b^* = 500\left(f\left(\frac{Y}{Y_0}\right) - f\left(\frac{Z}{Z_0}\right)\right) \end{cases}, \quad (18)$$

where, X, Y, and Z in (17) and (18) are defined in (16). Also, $X_0=Y_0=Z_0=255$.

$$CIE - LHC : \begin{cases} L^* = 116f\left(\frac{Y}{Y_0}\right) \\ H = \tan^{-1}\left(\frac{b^*}{a^*}\right) \\ C^* = \sqrt{a^{*2} + b^{*2}} \end{cases}, \quad (19)$$

where, Y comes from (16), $Y_0=255$, and a and b come from (18). In fact, CIE-LHC is the polar version of CIE-Lab [139]. The function f in (17), (18), and (19) is defined as [139]:

$$f(x) = \begin{cases} x^{\frac{1}{3}}, & x > 0.008856 \\ 7.787x + \frac{16}{116}, & otherwise. \end{cases} \quad (20)$$

$$YC_b C_r : \begin{cases} Y = 0.30R + 0.59G + 0.11B \\ C_b = 0.56(B - Y) \\ C_r = 0.71(R - Y) \end{cases}, \quad (21)$$

$$YIQ : \begin{cases} Y = 0.30R + 0.59G + 0.11B \\ I = 0.60R - 0.28G - 0.32B \\ Q = 0.21R - 0.52G + 0.31B \end{cases}, \quad (22)$$

$$YUV : \begin{cases} Y = 0.30R + 0.59G + 0.11B \\ U = -0.15R - 0.29G + 0.44B \\ V = 0.62R - 0.52G - 0.10B \end{cases}, \quad (23)$$

$$IR_g B_y : \begin{cases} I = L(G) \\ R_g = L(R) - L(G) \\ B_y = L(B) - \frac{L(R)+L(G)}{2} \\ L(x) = 105 \log_{10}(x + 1) \end{cases}, \quad (24)$$

$$IR_g B_y^+ : \begin{cases} I = L(G) \\ R_g = L(R) - L(G) \\ B_y = L(B) - \frac{L(R)+L(G)}{2} \\ L(x) = 105 \log_{10}(x + 1 + n) \end{cases}, \quad (25)$$

where, n is a uniform random variable in [0, 1].

$$Nrgb : \begin{cases} r = \frac{R}{R+G+B} \\ g = \frac{G}{R+G+B} \\ b = \frac{B}{R+G+B} \end{cases}, \quad (26)$$

which is essentially a 2-D color space.

$$YC_b C_r^\circ : \begin{cases} Y = 0.30R + 0.59G + 0.11B \\ I^\circ = \sqrt{C_b^2 + C_r^2} \\ Q^\circ = \tan^{-1} \frac{C_b}{C_r} \end{cases}, \quad (27)$$

which is the polar version of $YC_b C_r$, with C_b and C_r coming from (21).

$$YIQ^\circ : \begin{cases} Y^\circ = 0.30R + 0.59G + 0.11B \\ C_b^\circ = \sqrt{I^2 + Q^2} \\ C_r^\circ = \tan^{-1} \frac{I}{Q} \end{cases}, \quad (28)$$

which is the polar version of YIQ , with I and Q coming from (22).

$$YUV^\circ : \begin{cases} Y = 0.30R + 0.59G + 0.11B \\ U^\circ = \sqrt{U^2 + V^2} \\ V^\circ = \tan^{-1} \frac{U}{V} \end{cases}, \quad (29)$$

which is the polar version of YUV , with U and V coming from (23).

After these three polar color spaces, there are two cartesian color spaces, namely HSI^c and HSV^c , defined as:

$$HSI^c : \begin{cases} H^c = S \sin H \\ S^c = S \cos H \\ I^c = \frac{1}{3}(R + G + B) \end{cases} \quad (30)$$

where, H and S come from (13). Also, we have,

$$HSV^c : \begin{cases} H^c = S \sin H \\ S^c = S \cos H \\ V^c = \max(R, G, B) \end{cases} \quad (31)$$

where, H and S come from (14).

The ratio RGB is defined as:

$$RGBr : \begin{cases} Rr = \frac{R}{G} \\ Gr = \frac{G}{B} \\ Br = \frac{B}{R} \end{cases}, \quad (32)$$

which is a 2-D color space. Finally, *Tint-Saturation-Lightness* (TSL) color space is defined as:

$$TSL : \begin{cases} T = \begin{cases} \frac{1}{2\pi} \tan^{-1} \frac{r'}{g'} + \frac{1}{4}, & g' < 0 \\ \frac{1}{2\pi} \tan^{-1} \frac{r'}{g'} + \frac{3}{4}, & g' > 0 \\ 0, & g' = 0 \end{cases} \\ S = \sqrt{\frac{9}{5}(r'^2 + g'^2)} \\ L = 0.30R + 0.59G + 0.11B \\ r' = r - \frac{1}{3} \\ g' = g - \frac{1}{3} \end{cases}, \quad (33)$$

where r and g come from (26).

Almost all color spaces are (mostly, one-to-one) functions $F: (N_{255} \cup \{0\})^3 \rightarrow R^3$. For convenient we call the set $(N_{255} \cup \{0\})^3$ as Θ . In order to make the representation of different color spaces comparable, we perform a linear normalization scheme. As such, for each color space $F=[F_1, F_2, F_3]^T$ ($F_i: \Theta \rightarrow R$), the normalized color space \tilde{F} is defined as:

$$\tilde{F}(\vec{c}) = \begin{pmatrix} [\alpha_1 F_1 + \beta_1] \\ [\alpha_2 F_2 + \beta_2] \\ [\alpha_3 F_3 + \beta_3] \end{pmatrix}, \quad (34)$$

where, α_i and β_i are constant real values and $[x]$ denotes the integer value of x . The constants α_i and β_i are selected in the way that F turns into a $\Theta \rightarrow \Theta$ function, which is applicable for digital 8-bit processing. Table 5 lists the values of α_i and β_i for the color spaces stated above. It is clear that for a color component F we have

$$\alpha = \frac{255}{\max_{\vec{x} \in \Theta} \{F(\vec{x})\} - \min_{\vec{x} \in \Theta} \{F(\vec{x})\}}, \quad (35)$$

$$\beta = 255 \frac{-\min_{\vec{x} \in \Theta} \{F(\vec{x})\}}{\max_{\vec{x} \in \Theta} \{F(\vec{x})\} - \min_{\vec{x} \in \Theta} \{F(\vec{x})\}}. \quad (36)$$

In some cases that computing the global maximum and minimum values of a single color component was not practically possible, a fair approximation is used.

Table 6 lists the names of different color spaces used in this paper.

B. ROC Curves

Figures 13 and 14 show the ROC curves of the OLUT and BLUT-based skin detectors in the color spaces under examination, respectively.

Table 5 Normalization factors for color spaces under investigation.

Color Space	α_1	α_2	α_3	β_1	β_2	β_3
RGB	1	1	1	0	0	0
HMMD	$255/\pi$	1	1	0	0	0
$I_1 I_2 I_3$	1	1	1	$255/2$	$255/2$	0
HSI	$255/\pi$	255	1	0	0	0
CIE-XYZ	0.84	1	1	0	0	0
HSV	$255/(2\pi)$	255	1	0	0	0
$Yc_b C_r$	1	0.56	0.71	0	$255/2$	$255/2$
CIE-Lab	265.8	147.9	147.9	-40.8	$255/2$	$255/2$
YIQ	1	0.83	0.96	0	$255/2$	$255/2$
CIE-LHC	2.55	$-255/\pi$	$255/\sqrt{2}$	-40.8	$255/2$	0
YUV	1	1.14	0.81	0	$255/2$	$255/2$
CIE-Luv	2.55	0.58	0.78	-40.8	94	140
$I_r B_y$	1	0.5	0.5	0	$255/2$	$255/2$
$I_r B_y^+$	1	0.5	0.5	0	$255/2$	$255/2$
Nrgb	255	255	255	0	0	0
YUV°	1	1.32	$255/(2\pi)$	0	0	$255/2$
YIQ°	1	1.26	$255/(2\pi)$	0	0	$255/2$
$YCbCr^\circ$	1	0.88	$255/(2\pi)$	0	0	$255/2$
HSI^c	1	$255/2$	$255/2$	0	$255/2$	$255/2$
HSV^c	1	$255/2$	$255/2$	0	$255/2$	$255/2$
RGBr1	1	1	1	0	0	0
TSL	$2 \times 255/3$	$255\sqrt{5}/\sqrt{8}$	1	$255/6$	0	0

¹ The range of this color space spans $[0, \infty]$. Hence no linear normalization works on it.

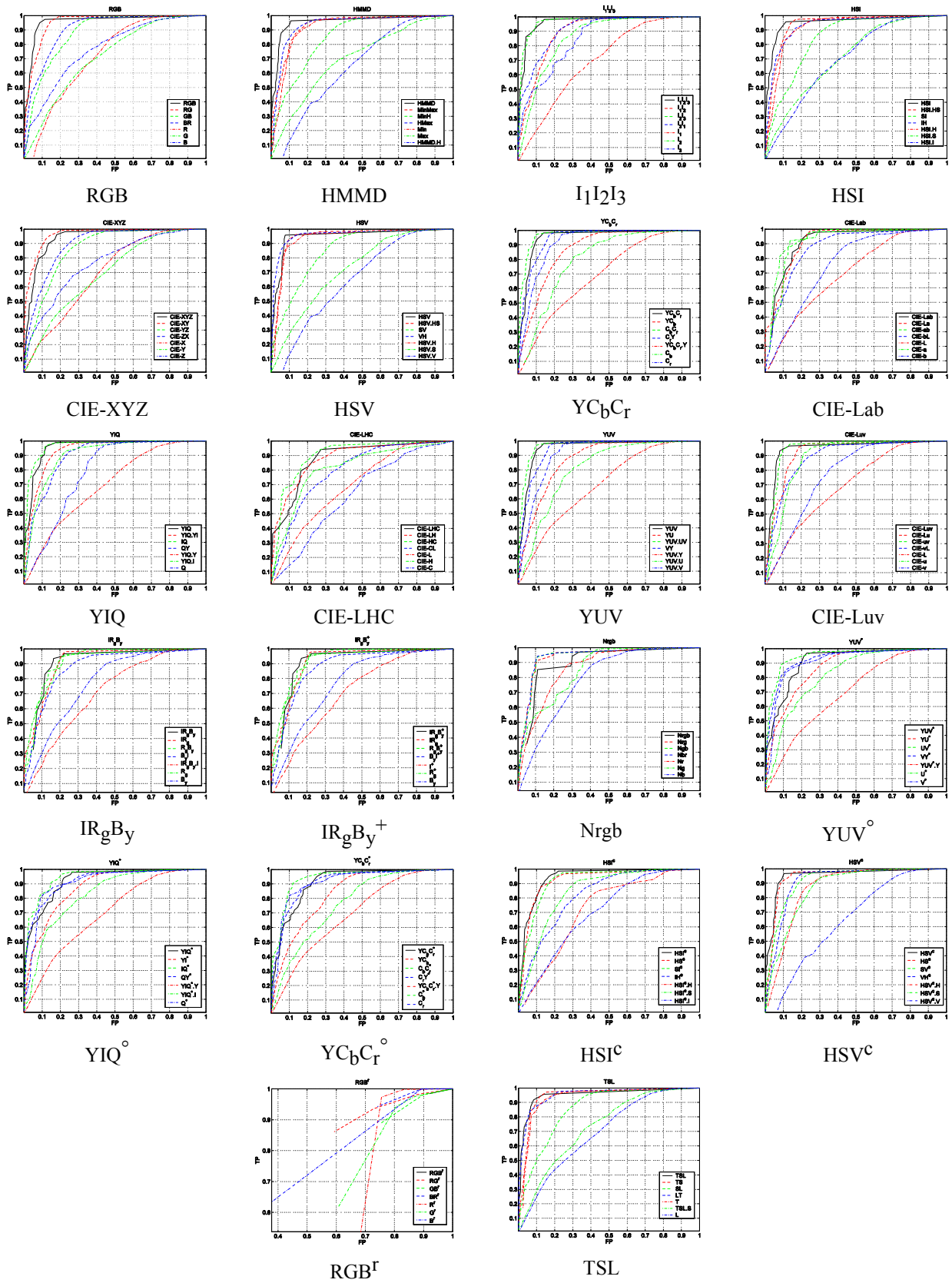


Fig. 13 ROC curves of the OLUT-based skin detector.

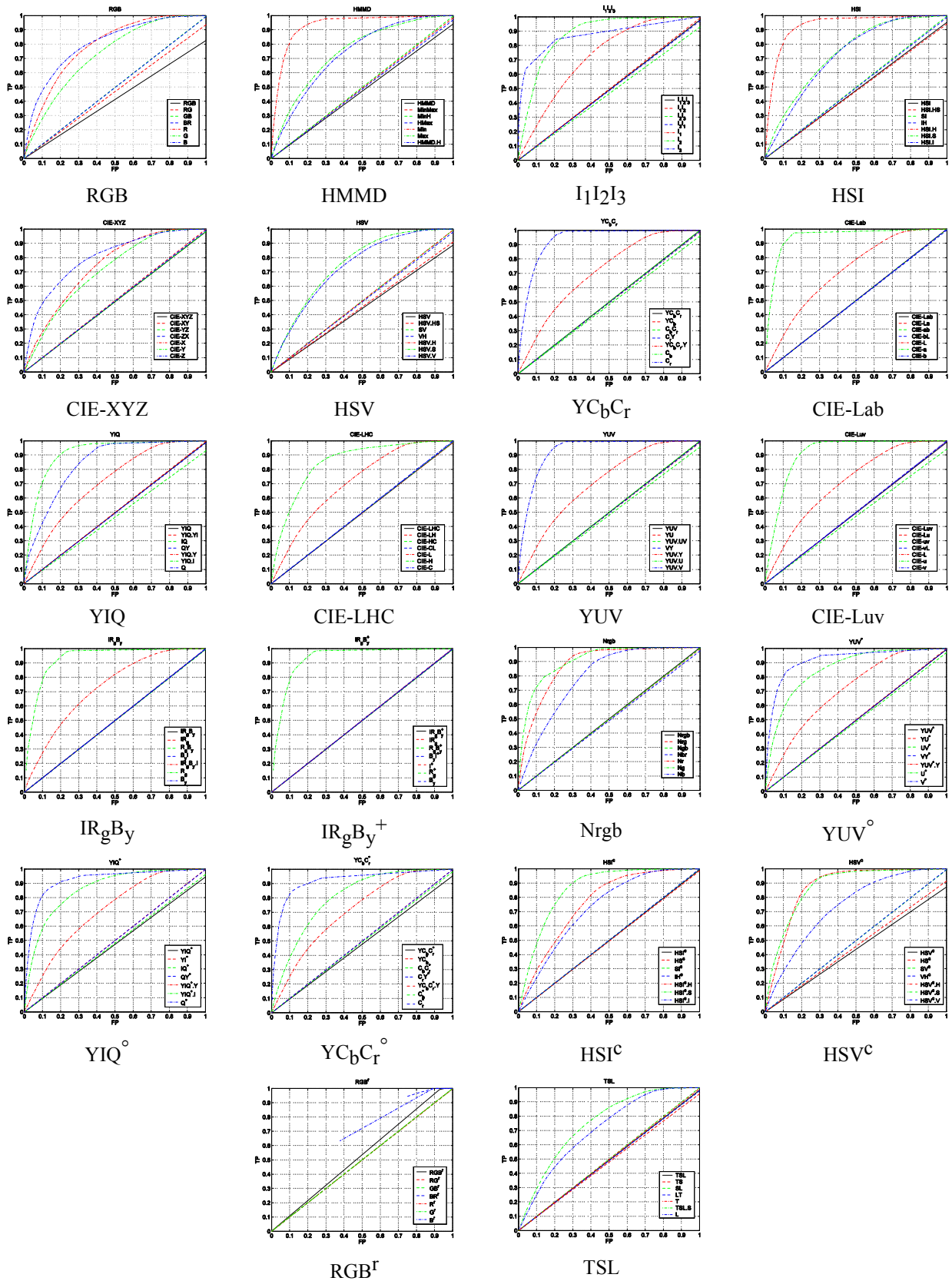


Fig. 14 ROC curves of the BLUT-based skin detection.

Table 6 Naming convention of color spaces and their representations.

Color Space	x_1x_2	x_2x_3	x_3x_1	x_1	x_2	x_3
HMMD	MinMax	MinH	HMax	Min	Max	HMMD.H
$I_1I_2I_3$	I_1I_2	I_2I_3	I_3I_1	I_1	I_2	I_3
HSI	HS	SI	IH	HSI.H	HSI.S	HSI.I
CIE-XYZ	CIE-XY	CIE-YZ	CIE-ZX	CIE-X	CIE-Y	CIE-Z
HSV	HS	SV	VH	HSV.H	HSV.S	HSV.V
YC_bC_r	YC_b	C_bC_r	C_rY	$YC_bC_r.Y$	C_b	C_r
CIE-Lab	CIE-La	CIE-ab	CIE-bL	CIE-L	CIE-a	CIE-b
YIQ	YIQ.YI	IQ	QY	YIQ.Y	YIQ.I	Q
CIE-LHC	CIE-LH	CIE-HC	CIE-CL	CIE-L	CIE-H	CIE-C
YUV	YU	YUV.UV	VY	YUV.Y	YUV.U	YUV.V
CIE-Luv	CIE-Lu	CIE-uv	CIE-vL	CIE-L	CIE-u	CIE-v
IR_gB_v	IR_g	R_gB_v	B_vI	$IR_gB_v.I$	R_g	B_v
$IR_gB_v^+$	IR_g^+	$R_gB_v^+$	B_vI^+	I^+	R_g^+	B_v^+
Nrgb	Nrg	Ngb	Nbr	Nr	Ng	Nb
YUV°	YU°	UV°	VY°	$YUV^\circ.Y$	U°	V°
YIQ°	YI°	IQ°	QY°	$YIQ^\circ.Y$	$YIQ^\circ.I$	Q°
$YC_bC_r^\circ$	YC_b°	$C_bC_r^\circ$	C_rY°	$YC_bC_r^\circ.Y$	C_b°	C_r°
HSI^c	HS^c	SI^c	IH^c	$HSI^c.H$	$HSI^c.S$	$HSI^c.I$
HSV^c	HS^c	SV^c	VH^c	$HSV^c.H$	$HSV^c.S$	$HSV^c.V$
RGB^f	RG^f	GB^f	BR^f	R^f	G^f	B^f
TSL	TS	SL	LT	T	TSL.S	L

References

[1] Ding C., Chi C.-H., Deng J. and Dong C.-L., "Centralized content-based web filtering and blocking: How far can it go," in *Proceeding of IEEE International Conference on Systems, Man and Cybernetics (SMC)*, 1999.

[2] Burke D., "Cybersmut and the first amendment: A call for a new obscenity standard," *Harvard Journal of Law & Technology*, 1996.

[3] "Internet pornography: Are children at risk?" <http://www.nap.edu/catalog/10261.html?onpi-webextra-050202>.

[4] Faucette J. E., "The freedom of speech and a frightened university's censorship of sex on the internet," *Duke Law Journal*, 1995.

[5] "Internet filter review," <http://www.internetfilterreview.com/internet-pornography-statistics.html>, 2003.

[6] WebsenseTM, "http://www.websense.com/products/resources/wp/hr_wp.pdf, 2003.

[7] "Family safe media," http://www.familysafemedia.com/pornography_statistics.html.

[8] Mehta M. D. and Plaza D., "Content analysis of pornographic images available on the internet," *The Information Society*, Vol. 13(2), pp. 153-161, 1997.

[9] Coopersmith J., "Pornography, videotape, and the internet," *IEEE Technology and Society Magazine*, Vol. Spring, pp. 27-34, 2000.

[10] Taylor M., Quayle E. and Holland G., "Child pornography, the internet and offending," *ISUMA - Canadian Journal of Policy Research*, Vol. 2(2), 2001.

[11] Krone T., "A typology of online child pornography offending," Australian Government, Australian Institute of Criminology, Trends and Issues in Crime and Criminal Justice, No. 279, www.ahtcc.gov.au, 2004.

[12] Day M. and Gehringer E., "Educators and pornography: the."

[13] Greenfield P., Rickwood P. and Tran H., "Effectiveness of internet filtering software products," CSIRO Mathematical and Information Science, 2001.

[14] "White house 'couples' set off indecency program," *Iowa City Press Citizen*, 1996.

[15] Starykevitch B. and Daoudi M., "Poesia software architecture definition document," http://www.poesia-filter.org/pdf/Deliverable_3_1.pdf, 2002.

- [16] Ho W. and Watters P., "Statistical and structural approaches to filtering internet pornography," in *IEEE International Conference on Systems, Man and Cybernetics*, 2004, pp. 4792-4798.
- [17] "Internet law and regulation," in *FT Tax & Law*, Smith G. J. H, Ed. London, UK, 1997, pp. 21-27.
- [18] Rimm M., "Marketing pornography on the information superhighway," *Georgetown Law Journal*, Vol. 83(5), pp. 1849-1934, 1985.
- [19] Elmer-DeWitt P., "Cyberporn," *Time magazine*, Vol. 146(1), pp. 1-10, 1995.
- [20] Grossman W. M., "net.wars," NYU Press, 1997.
- [21] Traynor I., "Child porn verdict stuns net lawyers," *The Guardian*, 1998.
- [22] Smith D., Harvey R., Chan Y. and Bangham J. A., "Classifying web pages by content," in *IEE European Workshop on Distributed Imaging*, Vol. 99/109, 1999, pp. 8/1-8/7.
- [23] Fleck M., Forsyth D. and Bregler C., "Finding naked people," in *European Conference on Computer Vision*, Buxton B. and Cipolla R., Eds. Berlin, Germany: Springer-Verlag, 1996, pp. 593-602.
- [24] Forsyth D. A. and Fleck M. M., "Identifying nude pictures," in *Third IEEE Workshop on the Applications of Computer Vision (WACV '96)*, Sarasoto, Florida, 1996, pp. 103-108.
- [25] Forsyth D. A. and Fleck M., "Automatic detection of human nudes," *International Journal of Computer Vision*, Vol. 32(1), pp. 63-77, 1999.
- [26] Ioffe S. and Forsyth D., "Finding people by sampling," in *IEEE International Conference on Computer Vision*, Corfu, Greece, 1999.
- [27] Ioffe S. and Forsyth D. A., "Probabilistic methods for finding people," *International Journal of Computer Vision*, Vol. 43(1), pp. 45-68, 2001.
- [28] Wang J. Z., Wiederhold G. and Firschein O., "System for screening objectionable images using daubechies' wavelets and color histograms," *Computer Communications*, Vol. 21(25), pp. 1355-1360, 1998.
- [29] Chan Y., Harvey R. and Smith D., "Building systems to block pornography," in *Challenge of Image Retrieval, BCS Electronic Workshops in Computing Series (CIR'99)*, Eakins J. and Harper D., Eds., Newcastle, 1999, pp. 34-40.
- [30] Chan Y., Harvey R. and Bagham J., "Using colour features to block dubious images," in *Proceedings of Eusipco 2000*, 2000.
- [31] Bosson A., Cawley G. C., Chan Y. and Harvey R., "Non-retrieval: Blocking pornographic images," in *Proceedings of International Conference on the Challenge of Image and Video Retrieval, Lecture Notes in Computer Science*, Vol. 2383. Springer-Verlag, 2002, pp. 60-70.
- [32] Jiao F., Gao W., Duan L. and Cui G., "Detecting adult image using multiple features," in *Proceedings of International Conferences on Info-tech and Info-net ICII'01*, Beijing, China, 2001, pp. 378-383.
- [33] Drimbarean A. F., Corcoran P. M., Cuic M. and Buzuloiu V., "Image processing techniques to detect and filter objectionable images based on skin tone and shape recognition," in *Proceedings of the International Conference on Consumer Electronics (ICCE)*, 2001, pp. 278-279.
- [34] Cao L.-L., Li X.-L., Yu H.-H. and Liu Z.-K., "Naked people retrieval based on adaboost learning," in *Proceedings of the First International Conference on Machine Learning and Cybernetics*, Beijing, China, 2002, pp. 1133-1138.
- [35] Jones M. J. and Rehg J. M., "Detecting adult images," HP Cambridge Research Laboratory, http://crl.research.compaq.com/projects/vision/adult_detection.html, 2002.
- [36] Jones M. J. and Rehg J. M., "Statistical color models with application to skin detection," in *Proceedings of Computer Vision and Pattern Recognition (CVPR'99)*, 1999, pp. 274-280.
- [37] Yoo S.-J., Jung M. ho, Kang H. B., Won C. S. and Choi S.-M., "Composition of mpeg-7 visual descriptors for detecting adult images on the internet," *Lecture Notes in Computer Science*, Vol. 2713, pp. 682-687, 2003.
- [38] Yoo S.-J., "Intelligent multimedia information retrieval for identifying and rating adult images," *Lecture Notes in Artificial Intelligence*, Vol. 3213, pp. 164-170, 2004.
- [39] Schettini R., Brambilla C., Cusano C. and Ciocca G., "On the detection of pornographic digital images," *Visual Communications and Image Processing*, Vol. 5150, pp. 2105-2113, 2003.
- [40] Lin Y.-C., Tseng H.-W. and Fuh C.-S., "Pornography detection using support vector machine," in *16th IPPR Conference on Computer Vision, Graphics and Image Processing (CVGIP 2003)*, Kinmen, ROC, 2003, pp. 123-130.
- [41] Hammami M., Chahir Y. and Chen L., "Webguard: Web based adult content detection and filtering system," in *Proceedings of the International Conference on Web Intelligence (WI'2003)*, 2003, pp. 574 - 578.

- [42] Hammami M., Tsishkou D. and Liming C., "Adult content web filtering and face detection using data-mining based skin-color model," in *Proceedings of the International Conference on Multimedia and Expo (ICME'04)*, 2004, pp. 403-406.
- [43] Jeong C.-Y., Kim J.-S. and Hong K.-S., "Appearance-based nude image detection," in *Proceedings of 17-th International Conference on Pattern Recognition (ICPR'04)*, Cambridge, UK, 2004.
- [44] Arentz W. A. and Olstad B., "Classifying offensive sites based on image content," *Computer Vision and Image Understanding*, Vol. 94, pp. 295-310, 2004.
- [45] Zheng H., Daoudi M. and Jedynek B., "Blocking adult images based on statistical skin detection," *Electronic Letters on Computer Vision and Image Analysis*, Vol. 4(2), pp. 1-14, 2004.
- [46] Zheng H., Liu H. and Daoudi M., "Blocking objectionable images: adult images and harmful symbols," in *Proceedings of IEEE International Conference on Multimedia and Expo*, Taipei, Taiwan, 2004.
- [47] Zheng H., Daoudi M. and Jedynek B., "Adult image filtering for web safety," in *Proceedings of 2nd International Symposium on Image/Video Communications Over Fixed and Mobile Networks*, Brest, France, 2004, pp. 77-80.
- [48] Zheng H., Daoudi M., Tombelle C. and Djeraba C., "Adult image filtering for internet safety," in *Multimedia Security Handbook*, Fuhr B. and Kirouski D., Eds. CRC Press, 2004.
- [49] Zheng H., "Maximum entropy modelling for skin detection: with an application to internet filtering," Ph.D. dissertation, University of Lille, France, 2004.
- [50] Zheng H., Daoudi M. and Jedynek B., "Adult image detection using statistical model," in *Compression et Représentation des Signaux Audiovisuels*, Lille, France, 2004.
- [51] Jinfeng Yang T. T. W. H., Fu Z., "A novel approach to detecting adult images," in *Proceedings of 17-th International Conference on Pattern Recognition (ICPR'04)*, Cambridge, UK, 2004.
- [52] Zheng Q.-F., Zeng W., Wen G. and Wang W.-Q., "Shape-based adult image detection," in *Proceedings of the Third International Conference on Image and Graphics*, 2004, pp. 150-153.
- [53] Rossoti H., *Colour: Why the World isn't Grey*. Princeton, NJ: Princeton University Press, 1983.
- [54] Yang M.-H., Kriegman D. J. and Ahuja M., "Detecting faces in images: A survey," *IEEE Transactions on Pattern Analysis and Machine Intelligence*, Vol. 24(1), pp. 34-58, 2002.
- [55] Jones M. J. and Rehg J. M., "Skin color modelling and detection," HP Cambridge Research Laboratory, <http://crl.research.compaq.com/projects/vision/>, 2002.
- [56] Brand J. D. and Mason J. S., "A comparative assessment of three approaches to pixel level human skin-detection," in *Proceedings of the International Conference on Pattern Recognition*, 2000, pp. 1056-1059.
- [57] Brand J. and Mason J., "A skin probability map and its use in face detection," in *IEEE International Conference on Image Processing (ICIP01)*, 2001, pp. 1034-1037.
- [58] Satoh S., Nakamura Y. and Kanade T., "Name-it: Naming and detecting faces in news videos," *IEEE Multimedia*, Vol. 6(1), pp. 22-35, 1999.
- [59] Jebara T. and Pentland A., "Parameterized structure from motion for 3d adaptive feedback tracking of faces," in *Proc. IEEE Conference Computer Vision and Pattern Recognition*, 1997, pp. 144-150.
- [60] Jebara T., Russell K. and Pentland A., "Mixtures of eigenfeatures for real-time structure from texture," in *Proc. Sixth IEEE International Conference on Computer Vision*, 1998, pp. 128-135.
- [61] Stern H. and Efros B., "Adaptive color space switching for face tracking in multi-colored lighting environments," in *Proceedings of the Fifth IEEE International Conference on Automatic Face and Gesture Recognition (FGR'02)*, 2002.
- [62] Quek F. K. H., Mysliwiec T. and Zhao M., "Fingermouse: A freehand computer pointing interface," in *Proceedings of the International Workshop on Automatic Face- and Gesture-Recognition*, Zurich, Switzerland, 1995, pp. 372-377.
- [63] Mysliwiec T. A., "Fingermouse: A freehand computer pointing interface," University of Illinois at Chicago, Tech. Rep. VISLab-94-01.
- [64] Phung S. L., Chai D. and Bouzerdoum A., "Adaptive skin segmentation in color images," in *Proceedings of the International Conference on Acoustics, Speech, and Signal Processing*, Hong Kong, 2003, pp. 173-176.
- [65] Irchfield S., "Elliptical head tracking using intensity gradients and color histograms," in *Proceedings of CVPR '98*, 1998, pp. 232-237.
- [66] Jordao L., Perrone M., Costeira J. and Santos-Victor J., "Active face and feature tracking," in

Proceedings of the 10th International Conference on Image Analysis and Processing, 1999, pp. 572-577.

- [67] Sigal L., Sclaroff S. and Athitsos V., "Estimation and prediction of evolving color distributions for skin segmentation under varying illumination," in *Proceedings of IEEE Conference on Computer Vision and Pattern Recognition*, 2000, pp. 152-159.
- [68] Zarit B. D., Super B. J. and Quek F. K. H., "Comparison of five color models in skin pixel classification," in *ICCV'99 Int'l Workshop on recognition, analysis and tracking of faces and gestures in Real-Time systems*, 1999, pp. 58-63.
- [69] Zarit B. D., "Skin detection in video images," Master's thesis, University of Illinois at Chicago, Chicago, 1999.
- [70] Zarit B. D., "Skin detection in video images," VISLab, University of Illinois at Chicago, Tech. Rep. VISLab-99-01.
- [71] McKenna S., Gong S. and Raja Y., "Modelling facial colour and identity with Gaussian mixtures," *Pattern Recognition*, Vol. 31, pp. 1883-1892, 1998.
- [72] Sobottka K. and Pitas I., "Segmentation and tracking of faces in color images," in *Proceedings of the Second International Conference on Automatic Face and Gesture Recognition*, 1996, pp. 236-241.
- [73] Sobottka K. and Pitas I., "Face localization and feature extraction based on shape and color information," in *Proceedings of the IEEE International Conference on Image Processing*, 1996, pp. 483-486.
- [74] Wang Y. and Yuan B., "Fast method for face location and tracking by distributed behavior-based agents," *IEE Proceedings on Vision, Image, and Signal Processing*, Vol. 149(3), pp. 173-178, 2002.
- [75] Herodotou N., Plataniotis K. and Venetsanopoulos A., "Automatic location and tracking of the facial region in color video sequences," *Signal Processing: Image Communication*, Vol. 14, pp. 359-388, 1999.
- [76] Kjeldsen R. and Kender J., "Finding skin in color images," in *Proceedings of the Second International Conference on Automatic Face and Gesture Recognition*, 1996, pp. 312-317.
- [77] Brown D., Craw I. and Lewthwaite J., "A som based approach to skin detection with application in real time systems," in *Proceedings of the British Machine Vision Conference*, Manchester, UK, 2001, pp. 491-500.
- [78] Gomez G., "On selecting colour components for skin detection," in *Proceedings of the ICPR*, 2000, pp. 961-964.
- [79] Zarit B. D. and Quek B. J. S. F. K., "Comparison of five color models in skin pixel classification," University of Illinois at Chicago, Tech. Rep. VISLab-99-07.
- [80] Saxe D. and Foulds R., "Toward robust skin identification in video images," in *Proceedings of the Second International Conference on Automatic Face and Gesture Recognition*, 1996, pp. 379-384.
- [81] Terrillon J.-C., Shirazi M. N., Sukamachi H. and Akamatsu S., "Comparative performance of different skin chrominance models and chrominance spaces for the automatic detection of human faces in color images," in *Proceedings of the International Conference on Face and Gesture Recognition*, 2000, pp. 54-61.
- [82] Graf H. P., Cosatto E., Gibbon D., Kocheisen M. and Petajan E., "Multi-modal system for locating heads and faces," in *Proceedings of the Second International Conference on Automatic Face and Gesture Recognition*, Killington, Vermont, 1996, pp. 88-93.
- [83] Feyrer S. and Zell A., "Detection, tracking, and pursuit of humans with an autonomous mobile robot," in *International Conference on Intelligent Robots and Systems 1999 (IROS '99)*, Kyongju, Korea, 1999, pp. 864-869.
- [84] Chen Q., Wu H. and Yachida M., "Face detection by fuzzy matching," in *Proceedings of the Fifth IEEE International Conference on Computer Vision*, 1995, pp. 591-596.
- [85] Wu H., Yokoyama T., Pramadihanto D. and Yachida M., "Face and facial feature extraction from color images," in *International Conference on Automatic Face and Gesture Recognition*, 1996, pp. 345-350.
- [86] Chen Q., Wu H. and Yachida M., "Face detection by fuzzy pattern matching," in *IEEE 5th International Conference on Computer Vision*, 1995, pp. 591-596.
- [87] Menser B. and Wien M., "Segmentation and tracking of facial regions in color image sequences," in *Proceedings of SPIE Visual Communications and Image Processing*, 2000, pp. 731-740.
- [88] Ahlberg J., "A system for face localization and facial feature extraction," Linkoping University, Tech. Rep. LiTH-ISY-R-2172, 1999.
- [89] Chai D. and Bouzerdoum A., "A Bayesian approach to skin color classification in ycbcr color space," in *Proceedings of IEEE Region Ten*

Conference, Vol. 2, Kuala Lumpur, Malaysia, 2000, pp. 421-424.

- [90] Albiol A., Torres L. and Delp E. J., "An unsupervised color image segmentation algorithm for face detection applications," in *Proceedings of the International Conference on Image Processing*, Thessaloniki, Greece, 2001, pp. 681-684.
- [91] Spors S. and Rabenstein R., "A real-time face tracker for color video," in *IEEE International Conference on Acoustics, Speech & Signal Processing (ICASSP)*, Utah, USA, 2001.
- [92] Wangand H. and Chang S.-F., "A highly efficient system for automatic face region detection in mpeg video," *IEEE Trans. Circuits and Systems for Video Technology*, Vol. 7(4), pp. 615-628, 1997.
- [93] Chai D. and Ngan K. N., "Locating facial region of a head-and-shoulders color image," in *Proceedings of the Third International Conference on Automatic Face and Gesture Recognition*, 1998, pp. 124-129.
- [94] Chai D., Phung L. and Bouzerdoum A., "Skin color detection for face localization in human-machine communications," in *International IEEE Symposium on Signal Processing and Its Application (ISSPA)*, Kuala Lumpur, Malaysia, 2001, pp. 343-346.
- [95] Phung S. L., Bouzerdoum A. and Chai D., "A novel skin color model in ycbcr color space and its application to human face detection," in *Proceedings of IEEE International Conference on Image Processing (ICIP'2002)*, 2002, pp. 289-292.
- [96] Hsu R.-L., Abdel-Mottaleb M. and Jain A. K., "Face detection in color images," *IEEE Trans. Pattern Analysis and Machine Intelligence*, Vol. 24(5), pp. 696-702, 2002.
- [97] Butler D., Sridharan S. and Chandran V., "Chromatic colour spaces for skin detection using gmms," in *Proceedings of the IEEE International Conference on Acoustics, Speech, and Signal Processing (ICASSP '02)*, 2002, pp. IV3620-IV3623.
- [98] Yang M.-H. and Ahuja N., "Detecting human faces in color images," in *Proceedings of the IEEE International Conference on Image Processing*, 1998, pp. 127-130.
- [99] Yang M. and Ahuja N., "Gaussian mixture model for human skin color and its application in image and video databases," in *Proceedings of the SPIE: Conf. on Storage and Retrieval for Image and Video Databases (SPIE 99)*, 1999, pp. 458-466.
- [100] Schumeyer R. and Barner K., "A color-based classifier for region identification in video," *Visual Communications and Image Processing*, Vol. 3309, pp. 189-200, 1998.
- [101] Cai J., Goshtasby A. and Yu C., "Detecting human faces in color images," in *International Workshop on Multi-Media Database Management Systems*, 1998, pp. 124-131.
- [102] Dai Y. and Nakano Y., "Extraction for facial images from complex background using color information and sgld matrices," in *Proceedings of the First International Workshop on Automatic Face and Gesture Recognition*, 1995, pp. 238-242.
- [103] Dai Y. and Nakano Y., "Face-texture model based on sgld and its application in face detection in a color scene," *Pattern Recognition*, Vol. 29(6), pp. 1007-1017, 1996.
- [104] Wang C. and Brandstein M., "Multi-source face tracking with audio and visual data," in *IEEE MMSP*, 1999, pp. 169-174.
- [105] Marques F. and Vilplana V., "A morphological approach for segmentation and tracking of human faces," in *International Conference on Pattern Recognition (ICPR'00)*, 2000, pp. 5064-5068.
- [106] Collobert M., Feraud R., Tournier G. L., Bernier D., Vaiallet J. E., Mahieux Y. and Collobert D., "Listen: A system for locating and tracking individual speakers," in *Proceedings of the International Conference on Automatic Face and Gesture Recognition*, 1996, pp. 283-288.
- [107] Saber E. and Tekalp A., "Frontal-view face detection and facial feature extraction using color, shape and symmetry based cost functions," *Pattern Recognition Letters*, Vol. 17(8), pp. 669-680, 1998.
- [108] Saber E., Tekalp A. M. and Knox K., "Automatic image annotation using adaptive color classification," in *Proceedings of Graphic Models and Image Processing*, 1996, pp. 115-126.
- [109] Yamada M., Ebihara K. and Ohya J., "A new robust method for extracting human silhouettes from color images," in *Proceedings of the Third International Conference on Automatic Face and Gesture Recognition*, Nara, Japan, 1998, pp. 528-533.
- [110] Feris R. S., de Campos T. E. and Junior R. M. C., "Detection and tracking of facial features in video sequences," *Lecture Notes in Artificial Intelligence*, Vol. 1793, pp. 197-206, 2002.
- [111] Kim S.-H. and Kim H.-G., "Face detection using multi-modal information," in *Fourth IEEE International Conference on Automatic Face and Gesture Recognition 2000*, Europole Atrium, Grenoble, France, 2000, p. 14.
- [112] Kim S.-H., Kim N.-K., Ahn S. C. and Kim H.-

- G., "Object oriented face detection using range and color information," in *Proceedings of the Third International Conference on Automatic Face and Gesture Recognition*, 1998, pp. 76-81.
- [113] Sun Q., Huang W. and Wu J., "Face detection based on color and local symmetry information," in *Proceedings of the Third International Conference on Automatic Face and Gesture Recognition*, 1998, pp. 130-135.
- [114] Qian R., Sezan M. and Matthews K., "A robust real-time face tracking algorithm," in *Proceedings of IEEE International Conference on Image Processing*, 1998, pp. 131-135.
- [115] Miyake Y., Saitoh H., Yaguchi H. and Tsukada N., "Facial pattern detection and color correction from television picture for newspaper printing," *Imaging Technology*, Vol. 16(5), pp. 165-169, 1990.
- [116] Oliver N., Pentland A. and Berard F., "Lafer: Lips and face real time tracker," in *Proc. IEEE Conf. Computer Vision and Pattern Recognition*, 1997, pp. 123-129.
- [117] Crowley J. and Bedrune J., "Integration and control of reactive visual processes," in *Proceedings of the Third European Conference on Computer Vision*, Vol. 2, 1994, pp. 47-58.
- [118] Crowley J. and Berard F., "Multi-modal tracking of faces for video communications," in *Proceedings of the IEEE Conference on Computer Vision and Pattern Recognition*, 1997, pp. 640-645.
- [119] Yang J. and Waibel A., "A real-time face tracker," in *Proceedings of the Third Workshop Applications of Computer Vision*, 1996, pp. 142-147.
- [120] Yang J. and Waibel A., "Tracking human faces in real-time," Carnegie Mellon University, Tech. Rep. CMU-CS-95-210, 1995.
- [121] Starner T. and Pentland A., "Real-time asl recognition from video using hmm's," Media Lab, Massachusetts Institute of Technology, Tech. Rep. 375, 1996.
- [122] Shiele B. and Waibel A., "Gaze based tracking based on face-color," *International Workshop on Automatic Face- and Gesture-Recognition*, 1995.
- [123] Subutai A., "A usable real-time 3d hand tracker," in *Conference Record of the Asilomar Conference on Signals, Systems and Computers*, 1994, pp. 1257-1261.
- [124] Hunke M. and Waibel A., "Face locating and tracking for human-computer interaction," in *IEEE Computer*, 1994, pp. 1277-1281.
- [125] Farrukh A., Ahmad A., Khan M. I. and Khan N., "Automated segmentation of skin-tone regions in video sequences," in *Proceedings of the IEEE Students Conference, ISCON '02.*, Vol. 1, 2002, pp. 122-128.
- [126] Wark T. and Sridharan S., "A syntactic approach to automatic lip feature extraction for speaker identification," in *ICASSP*, 1998, p. 3693-3696.
- [127] Terrillon J.-C., David M. and Akamatsu S., "Automatic detection of human faces in natural scene images by use of a skin color model and of invariant moments," in *Proceedings of the 3rd. International Conference on Face & Gesture Recognition*, 1998, p. 112.
- [128] Shin M. C., Chang v and Tsap L. V., "Does color space transformation make any difference on skin detection?" in *IEEE Workshop on Applications of Computer Vision*, Orlando, FL, 2002, pp. 275-279.
- [129] Jayaram S., Schmutge S., Shin M. C. and Tsap L. V., "Effect of color space transformation, the illuminance component, and color modelling on skin detection," in *2004 IEEE Computer Society Conference on Computer Vision and Pattern Recognition (CVPR'04)*, 2004.
- [130] Albiol A., Torres L. and Delp E., "Optimum color spaces for skin detection," in *Proceedings of the International Conference on Image Processing*, 2001, pp. 122-124.
- [131] Vladimir Vezhnevets V. S. and Andreeva A., "A survey on pixel-based skin color detection techniques," in *GraphiCon'2003*, Moscow, Russia, 2003.
- [132] Chai D. and Ngan N., "Face segmentation using skin color map in video phone applications," *IEEE Transactions on CSVT*, Vol. 9(4), pp. 551-564, 1999.
- [133] Garcia C. and Tziritas G., "Face detection using quantized skin color regions merging and wavelet packet analysis," *IEEE Transactions on Multimedia*, Vol. 1(3), pp. 264-277, 1999.
- [134] Nojic N. and Pang K. K., "Adaptive skin segmentation for head and shoulder video sequence," in *SPIE VCIP'2000*, Perth, Australia, 2000.
- [135] Manjunath B., Ohm J.-R., Vasudevan V. and Yamada A., "Color and texture descriptors," *IEEE Transaction on Circuits and Systems for Video Processing*, Vol. 11 No. 6, pp. 703-715, 2001.
- [136] Tenenbaum J., Garvey T., Weyl S. and Welf H., "An interactive facility for scene analysis research," Stanford Research Institute, AI Center, Tech. Rep. 87, 1974.

- [137] J. Foley and A. Van Dam, *Fundamentals of Interactive Computer Graphics, The System Programming Series*,. Reading, MA.: Addison-Wesley, 1982, Reprinted 1984 with corrections.
- [138] Y. I. Ohta, Y. Kanade, and T. Saki, "Color information for region segmentation," *Computer Graphics and Image Processing*, Vol. 13, No.3, pp. 222-241, 1980.
- [139] Levkowitz H. and Herman G., "Color scales for image data," *IEEE Computer Graphics and Application*, 1992.
- [140] *ITU-R Recommendation BT-601-5: Studio Encoding Parameters of Digital Television for Standard 4:3 and Widescreen 16:9 Aspect Ratios*. Geneva: <http://www.itu.ch/>, 1994.
- [141] Benson K., *Television Engineering Handbook*, J. C. Whitaker, Ed. New York, London: Mc Graw-Hill, 1992.
- [142] Slater J., *Modern Television System to HDTV and Beyond*. London: Pitman, 1991.
- [143] Gershon R., Jepson A. D. and Tsotsos J. K., "Ambient illumination and the determination of material changes," *Journal of Optical Society of America*, Vol. A-3(10), pp. 1700-1707, 1986.
- [144] Chen Q., WU H. and Yachida M., "Face detection by fuzzy pattern matching," in *Proceedings of the Fifth International Conference on Computer Vision*, 1995, pp. 591-597.
- [145] Soriano M., Huovinen S., Martinkauppi B. and Laaksnoen M., "Skin detection in video under changing illumination conditions," in *Proceedings of the 15th International Conference on Pattern Recognition*, 2000, pp. 839-842.
- [146] Branscomb A. W., "Internet Babylon? Does the Carnegie Mellon study of pornography on the information superhighway reveal a threat to the stability of society?" *Georgetown Law Journal*, 1995.
- [147] Borns R. J., "The internet: Privacy, the first amendment, and transnational communications; what's at stake," in *Proceedings of FIE'96*, 1996, pp. 1337-1341.